This article has been accepted for publication in IEEE Access. This is the author's version which has not been fully edited and content may change prior to final publication. Citation information: DOI 10.1109/ACCESS.2025.3604649

IEEE Access
Multidisciplinary | Rapid Review | Open Access Journal

Date of publication xxxx 00, 0000, date of current version xxxx 00, 0000.

Digital Object Identifier 10.1109/ACCESS.2024.Doi Number

Fuzzy Fitness Distance Balance Gradient-Based Optimization Algorithm (fFDBGBO): An Application to Design and Performance Optimization of PMSM

Hasan Uzel[1], Yunus Hınıslıoğlu[2], Adem Dalcalı[3], and Uğur Güvenç[2]

[1]Akdağmadeni Vocational Schools, Department of Electric and Energy, Yozgat Bozok University, Yozgat 66900 TÜRKİYE
[2]Faculty of Engineering, Department of Electrical and Electronics Engineering, Düzce University, Düzce 81620 TÜRKİYE
[3]Faculty of Engineering and Natural Sciences, Department of Electrical and Electronics Engineering, Bandırma Onyedi Eylül University, Balıkesir 10200 TÜRKİYE

Corresponding author: Uğur Güvenç (ugurguvenc@duzce.edu.tr).

ABSTRACT The exceptional properties of Permanent Magnet Synchronous Motors (PMSMs), including their small construction, high power-torque density, and high efficiency, make them one of the most popular electrical machines. However, the motor structure needs to be optimized for circumstances like boosting the PMSM's energy efficiency, optimizing output power, and lowering motor weight and cogging torque. This research aims to identify the optimal values for the parameters essential to achieving the most efficient design of a 15 kW PMSM. For this purpose, a new optimization algorithm is proposed. This proposed algorithm is an application of the fuzzy logic-based fitness distance balance design to the gradient-based optimization algorithm (GBO). The developed algorithm is called fuzzy Fitness Distance Balance Gradient-Based Optimization (fFDBGBO) algorithm. The proposed algorithm and various optimization algorithms with effective results in the literature were tested for the fitness function determined to find the optimal values of Embrace, Offset, Skew Width, Magnet Thickness, and slot bottom width (Bs1) of PMSM. The results indicate that the suggested algorithm achieves better performance than rival algorithms in terms of effectiveness. Compared to the GBO algorithm, the proposed fFDBGBO method achieves a 0.2979% increase in efficiency. Compared to other algorithms, the suggested algorithm's objective function has the highest slot fill factor (49.9995%), yet it still complies with the specified limit value. Relative to the initial design, the motor efficiency achieved with the fFDBGBO algorithm improved from 91.7788% to 93.0366%, while the magnet weight decreased from 2.14837 to 2.09475, and the total motor weight remained approximately the same as 53.2286 kg and 54.0436 kg.

INDEX TERMS Permanent Magnet Synchronous Motor; Motor Parameter Optimization; Gradient-based Optimization; Fuzzy Fitness Distance Balance

I. INTRODUCTION

From production to consumption, electrical energy must be used efficiently and with excellent quality at every stage. Nowadays, a significant portion of the electrical energy generated is used by electric motors. Designs that will enable electric motors to operate with high efficiency need to be made in order to save energy. In PMSM, the rotor magnetic field is created by permanent magnets, which form no copper losses on the rotor and this leads to high motor efficiency. PMSMs provide numerous benefits, including low energy loss, compact design, high torque density, and excellent efficiency, particularly when integrated with driver technology and rare earth elements. [1]. The development happening in the magnet industry brings permanent magnet machines to the fore. PMSMs are motors that can be driven directly at low speeds without the need for a gear case. Due to these advantages, PMSMs are extensively utilized across multiple domains such as automotive, especially electric and hybrid vehicles, aircraft, marine, space, medicine, electrical home appliances, mill, paper, servo, and robotic applications [2],[3].

The optimization of PMSMs is a challenging task due to the need to consider multiple design criteria simultaneously. Simultaneous optimization of machine performance, cost, and other constraints expands the decision space and

This work is licensed under a Creative Commons Attribution 4.0 License. For more information, see https://creativecommons.org/licenses/by/4.0/

This article has been accepted for publication in IEEE Access. This is the author's version which has not been fully edited and
content may change prior to final publication. Citation information: DOI 10.1109/ACCESS.2025.3604649

increases the complexity of the solution process. Traditional analytical design methods, while useful, offer limited flexibility and heavily rely on user experience. These constraints often restrict the range of feasible design solutions. In recent years, soft computing techniques such as Genetic Algorithms (GA) and Artificial Neural Networks (ANN) have emerged as powerful tools for addressing these challenges. These methods enable the rapid development of unconventional and efficient designs by optimizing geometrical parameters beyond the capabilities of classical approaches [4].

In the design of electric motors, the highest power is tried to be obtained with minimum volume and minimum material usage. Researchers are working on optimum motor designs for PMSMs to operate more efficiently [5]. Usually, in these designs, PMSMs focus on different goals, such as increasing efficiency, reducing motor weight, torque ripple, and cogging torque. In these carried out studies, artificial intelligence-based optimization techniques are preferred in design due to the non-linear complex structures of PMSMs [6].

To enhance key performance metrics such as motor weight, efficiency, cogging torque, and power losses, optimizing geometric parameters is crucial. In recent years, designers have increasingly employed heuristic optimization algorithms to achieve these improvements [7]. In the study conducted by Duman and Dalcalı, TLBO, TLSBO, INFO, JSOA, and POA heuristic optimization methods were employed to optimize the stator slot structure and magnet geometry in a permanent magnet synchronous generator. In their study, the authors addressed the reduction of cogging torque and mitigation of total harmonic distortion in the PMSG. However, no improvement was made in the efficiency of the PMSG [8].

In a similar study, an enhanced multi-objective hummingbird-inspired optimization method (EMOHA) was utilized to suppress torque pulsations and boost the generated torque of the Embedded Magnet Synchronous Motor. Within this research, the machine parameters requiring optimization were identified using the Taguchi-based methodology and Surface Response Modeling (SRM) and subsequently refined with an advanced multi-goal metaheuristic inspired by hummingbirds. The optimized version of the motor provided a 0.33% increase in average torque while reducing torque ripple by 72.77% [9].

Sun et al., present a comprehensive multi-objective optimization strategy for a 12/10 pole switched reluctance motor (SRM) intended for electric vehicle applications. Their study integrates a Kriging-based surrogate modeling framework with the NSGA-II multi-objective genetic algorithm to efficiently explore the design space. The optimization focuses on improving key performance indicators such as output torque, torque ripple, stator and coil temperatures, and total losses. By considering both electromagnetic and thermal aspects within a unified framework, the study highlights the effectiveness of multiphysics and multidisciplinary optimization techniques in the design of SRMs. The findings underline the potential of advanced optimization algorithms to significantly enhance motor performance under practical constraints [10]. In contrast, Mahmouditabar and Baker focused on the design optimization of an induction motor (IM) by explicitly incorporating drive cycle performance. The optimization was based on three main criteria (efficiency, power factor, and rotor losses) and was conducted using the Design of Experiment (DOE)-based Taguchi method. A k-means clustering technique was applied to identify representative working points across various driving cycles. However, the study emphasized that the k-means method may fail to capture certain critical design regions, potentially overlooking feasible solutions that comply with the motor's performance envelope [11].

In conventional electric machine design processes, the simultaneous optimization of continuous and discrete variables is often limited due to computational burden and modeling complexity. As a solution to this challenge, the design optimization of interior permanent magnet (IPM) motors is addressed as a multi-objective optimization problem. In the study by Asanuma and Kanno, a novel framework is proposed where the computational burden of repeated electromagnetic analyses is alleviated by employing Radial Basis Function (RBF)-based surrogate modelling. This surrogate is then integrated into a Sequential Approximate Optimization (SAO) process, which is further enhanced by the Alternating Direction Method of Multipliers (ADMM) [12]. Optimum design parameters are optimized with the ABC algorithm to obtain high dynamic performance by reducing the mechanical time constant and electrical time constant in a PMSM designed for electric vehicles [13]. In the research conducted for hydrogen-powered electric vehicles, an advanced approximation-based multi-objective optimization approach has been introduced to minimize torque oscillations and reduce magnet consumption in embedded magnet synchronous motors. However, a significant amount of sampling and data is initially needed to build the model [14].

The Genetic Algorithm (GA) was implemented to reduce the overall cost and enhance the torque output of the transverse flux permanent magnet motor designed for electric bicycles. Nevertheless, within this research, the effectiveness of the suggested algorithm has not been evaluated against other optimization techniques [15]. In 2020, a study conducted by Yilmaz and colleagues utilized the Symbiotic Organisms Search (SOS) algorithm to refine the design parameters of PMSM. As a result of the optimization process, it was aimed to increase the efficiency and this was successful. However, in the study, the SOS algorithm was only compared with the Artificial

This work is licensed under a Creative Commons Attribution 4.0 License. For more information, see https://creativecommons.org/licenses/by/4.0/

This article has been accepted for publication in IEEE Access. This is the author's version which has not been fully edited and
content may change prior to final publication. Citation information: DOI 10.1109/ACCESS.2025.3604649

Bee Colony algorithm (ABC) [16]. In 2022, Ahandani et al. proposed two refined versions of the particle swarm optimization (PSO) approach for identifying PMSM parameters. The first, a quasi-oppositional PSO (QOPSO), exhibited superior computational efficiency. The second, a hybrid chaotic PSO (HCPSO), was found to deliver high-quality solutions. The HCPSO variant was benchmarked against five nature-inspired optimization methods from prior studies [17]. In 2012, Mutluer and Bilgin used PSO and GA to optimize the geometrical design parameters of PMSM. The optimizations performed compared both algorithms and it was observed that the efficiency increased in both algorithms. However, no algorithm was developed or improved in the study, only two algorithms were compared. However, in the study, no algorithm was developed or improved, only two algorithms were compared [6].

A review of the studies reveals that heuristic optimization algorithms are of great importance in determining the optimal parameters required for the design. Therefore, the algorithm to be selected must be effective. The gradient-based algorithm (GBO) [18], proposed by Ahmadianfar et al. and based on Newton's search method, was preferred in this study. In the GBO algorithm, solution candidates that will guide the search process are selected from the population by using the greedy selection method. However, due to this method, diversity disappears quickly. In order to address this issue with the GBO algorithm, various methods have been tried in the literature. One of these is the Chaotic Gradient-Based Optimizer algorithm, which aims to improve the algorithm using chaotic maps. In the study conducted by Abd Elminaam and his team in 2022, ten different chaotic maps were utilized to reduce the likelihood of the GBO algorithm getting stuck in local points and converging early, thereby increasing its efficiency. To measure the effectiveness of the obtained CGBO algorithm, comparisons were made with the PSO, moth flame optimizer (MFO), sine cosine algorithm (SCA), salp swarm algorithm (SSA), and GBO algorithms found in the literature [19]. In this study, to eliminate the problem of early loss of diversity and increase efficiency, the fuzzy fitness distance balance (fFDB) method was used to develop the GBO algorithm. The Fitness-Distance Balance (FDB) approach serves as a selection mechanism aimed at enhancing the search efficiency of MHS-based algorithms [20]. Nonetheless, refinements are required in the technique employed for computing the FDB score within this framework [21]. Consequently, this research adopts a fuzzy logic-based strategy for determining the FDB score.

As a result, the structural optimization of the PMSM motor was carried out in this study. During the design phase, a fuzzy logic-based fitness-distance balance approach was applied to the GBO algorithm. The primary contributions of this study can be summarized as follows:

- A novel perspective is introduced into the GBO algorithm through the application of the fFDB selection strategy. As a result, a powerful fuzzy-Fitness Distance Balance-Gradient Based Optimization (fFDBGBO) algorithm was developed.
- In the design of PMSM, five different parameters were simultaneously considered as variables. The stator slot structure parameters include stator slot skew and bottom width, while the magnet structure parameters consist of magnet thickness, pole embrace, and offset.
- For the optimization problem, five input variables are optimized, and a single objective function is introduced that simultaneously integrates three output parameters—Efficiency, Stator Slot Fill Factor, and Output Power.
- For the first time, the suggested algorithm was utilized to solve the problem, and its performance was benchmarked against several well-established optimization algorithms from the literature, including INFO, GA, PSO, ARO, DE, LSHADE, SNS, jDE, SaDE, BBO, JADE, and GBO.

The following sections of the paper can be stated as follows: Definition of the problem, control variable explanations, and objective function are defined in Section 2. A detailed description of GBO, fFDB method and the developed fFDBGBO algorithm, which form the basis of the proposed algorithm, is given in Section 3. The results obtained from all simulations and benchmarks with other algorithms are given in Section 4. Conclusions and recommendations are given in the last section.

II. MATERIALS AND METHODS

The performance of electric machines is directly related to their geometric structure. The configuration and positioning of the stator, rotor, and magnets significantly influence the machine's magnetic and electrical equivalents, thereby affecting its overall performance [22]. The five optimization parameters considered in this study (Embrace, Offset, Skew, Magnet Thickness, and Slot Bottom Width (Bs1)) were selected based on their direct and critical impact on the performance of PMSMs. Moreover, these parameters are commonly encountered as key optimization variables in both literature and industrial applications. The "Embrace" allows the optimization of cogging torque and back-emf waveform. By adjusting the "Offset", the air gap flux waveform can be optimized, thereby improving both motor efficiency and cogging torque. The "Skew" is essential for minimizing cogging torque through axial slot displacement. "Magnet Thickness" enables torque- and cost-oriented optimizations by controlling magnetic flux levels and magnet mass. "Bs1", which determines the stator slot geometry, directly influences the current-carrying capacity and consequently copper losses, thereby affecting motor performance.

These parameters were selected based on electromagnetic analyses, engineering experience, and prior studies in

This work is licensed under a Creative Commons Attribution 4.0 License. For more information, see https://creativecommons.org/licenses/by/4.0/

This article has been accepted for publication in IEEE Access. This is the author's version which has not been fully edited and
content may change prior to final publication. Citation information: DOI 10.1109/ACCESS.2025.3604649

literature. Their minimum and maximum values (as defined in Table II) were established by taking into account geometric constraints and feasibility design. Altogether, these variables form a systematic optimization framework aimed at improving key performance metrics such as efficiency, torque generation, and total machine weight in PMSM design.

A. PMSM MOTOR DESIGN

The structures of PMSMs generally consist of stator, windings, permanent magnets, rotor, and shaft. The geometrical structure of PMSM is given in Figure 1.

A typical PMSM comprises a stator that includes phase windings, a rotor embedded with permanent magnets, and a shaft. Figure 1 illustrates a sectional representation of an example PMSM with an internal rotor. As shown in Figure 1, D_{so} represents the stator's outer diameter (mm), D denotes the stator's inner diameter (mm), D_{ro} refers to the rotor's outer diameter (mm), D_{ri} corresponds to the rotor's inner diameter (mm) and L signifies the stack length (mm).

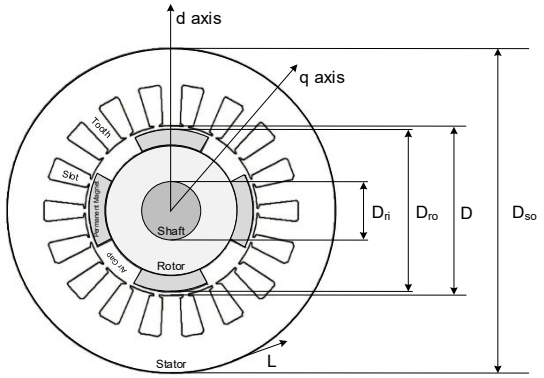

FIGURE 1. Geometry of PMSM.

Multiple criteria need to be considered together in the design of the PMSM. Correct material selection and optimum design can improve the performance of the PMSM. The analytical design of the PMSM can be started with the dimensioning equation given in Equation (1) [23].

$$S = 11.k_w.\bar{B}.ac.\left(\frac{D_{so}}{1000}\right)^2.\frac{L}{1000}.n_s \quad (1)$$

Here, S denotes the apparent power (VA), k_w represents the winding factor, $\bar{B}$ corresponds to the specific magnetic loading (T), and ac refers to the specific electrical loading (At/m), all of which are influenced by the nominal power, voltage and frequency. n_s epresents the rated speed of the motor (rpm). As can be seen from Equation (1), the stator outer diameter and stack length directly affect the power of the machine. The efficiency Eff of PMSM depends on the total power loss (P_{loss}) and the output power (P_{out}) as shown in Equation (2). The total power loss which is given in Equation (3) is the sum of copper losses (P_{cu}), iron losses (P_{core}), wind and friction losses $(P_{w\&f})$.

$$Eff = P_{out}/(P_{out} + P_{loss}) \quad (2)$$

$$P_{loss} = P_{cu} + P_{core} + P_{w\&f} \quad (3)$$

The magnetic flux density in the stator teeth and core is one of the primary factors influencing iron losses. The stator tooth flux density B_{st} can be found using Equation (4).

$$B_{st} = \Phi_{tm}/(T_{sw}.L.l_f) \quad (4)$$

In this equation, Φ_{tm} denotes the peak flux in the stator tooth, T_{sw} represents stator tooth width, and l_f donetes the lamination factor. The slot fill ratio is directly dependent on the slot area and physical structure of the machine. This ratio plays an important role in the formation of flux density as well as determining the number of conductors in the slot. A higher slot fill ratio generally results in an increase in the current capacity of the windings, which affects the performance and efficiency of the machine. Accordingly, the slot fill ratio is;

$$f_f = (6.N_c.A)/(N_s.A_s) \quad (5)$$

In this equation, A represents the cross-section of the conductor, N_c represents the turns per phase, N_s, A_s represents the slots number and area, respectively [23], [24]. The initial parameters of the PMSM designed in this study are given in Table I.

TABLE I
GEOMETRIC PARAMETERS OF THE DESIGNED PMSM

Parameters	Value
Number of poles	4
Rotor type	Inner/surface type
Stator outer/inner diameter (mm)	296.5/154.8
Rotor outer/inner diameter (mm)	152.8/60
Number of slots	24
Stack Length (mm)	113.9
Material of stator	M15
Material of rotor	M15
Material of magnet	N36
Embrace	0.72
Magnet thickness (mm)	8.72
Offset (mm)	14.5
Skew	0

1) PMSM VARIABLES

Electrical machine design is a complex and time-consuming process in which electromagnetic, mechanical, and thermal problems are considered together. We can evaluate the correct design of the magnetic circuit, the proper selection of conductors, and the magnetic saturation of the material used within electromagnetic constraints. Mechanical and thermal problems affect the durability, reliability, and duty cycle of the motor [8]. The choice of material affects the performance and durability of the motor; taking all these factors into consideration ensures that the desired performance is provided at an affordable cost and an industrial product emerges. Performing all these analyses requires making intensive effort and lengthy analyses. The study placed particular emphasis on key design parameters of the motor, including its embrace, magnet thickness, offset, skew, and stator slot structure. Table II shows the initial design values determined for the

This work is licensed under a Creative Commons Attribution 4.0 License. For more information, see https://creativecommons.org/licenses/by/4.0/

This article has been accepted for publication in IEEE Access. This is the author's version which has not been fully edited and
content may change prior to final publication. Citation information: DOI 10.1109/ACCESS.2025.3604649

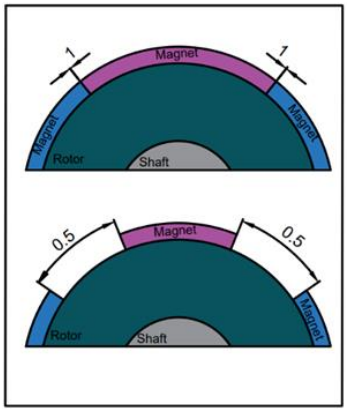

(a)

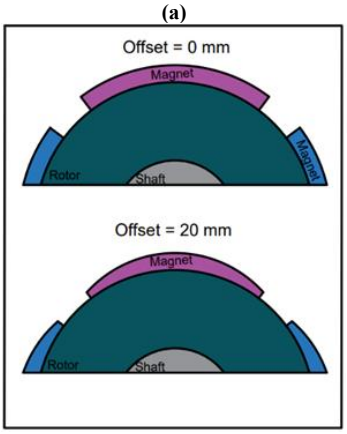

(b)

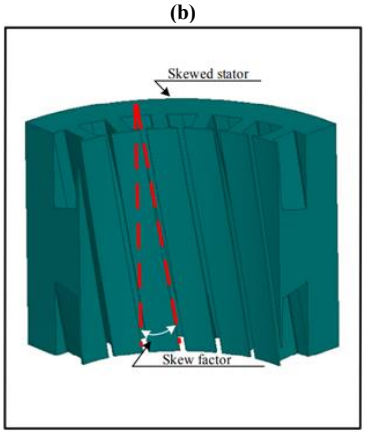

(c)

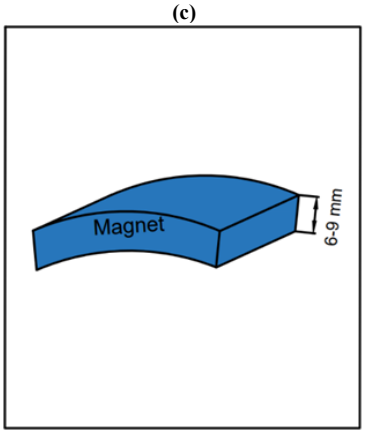

(d)

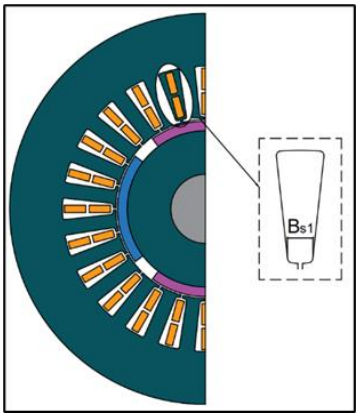

(e)

FIGURE 2. Geometry of optimization parameters of PMSM: (a) Embrace; (b) Offset; (c) Skew [25]; (d) Magnet Thickness; (e) Slot bottom width of stator slot (Bs1).

optimisation parameters of the PMSM and the minimum and maximum limits of these values.

Other design parameters of the machine, other than the variables presented in Table II, were kept constant and the variables presented in Table II are analysed between the specified minimum and maximum limits.These limit values were determined by considering user experience as well as geometric limits. Figure 2 provides the lower and upper values for the variables as well as the defined magnet parameters.

TABLE II
OPTIMIZATION PARAMETERS AND LIMITS

Index	Variable	Initial	Min. value	Max. value
X1	Embrace	0.93	0.5	1
X2	Offset (mm)	0.079	0	20
X3	Skew	0.85	0	1
X4	Magnet Thickness (mm)	8.95	6	9
X5	Bs1 (mm)	5.90	5	9

- Embrace

Embrace is characterized as the ratio of the pole arc length to the pole spacing [25]. The magnet embrace ratio is calculated by Equation (6).

$$Embrace = \frac{Pole\ Arc}{Pole\ Pitch} \tag{6}$$

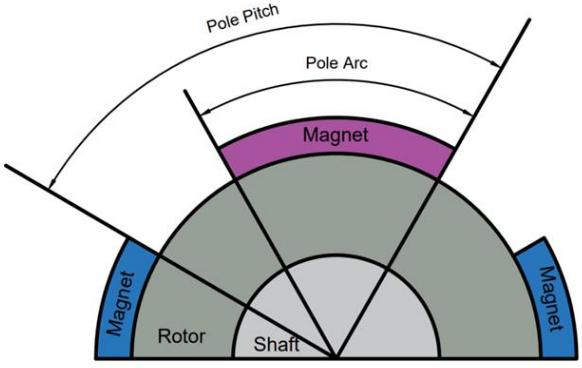

FIGURE 3. Permanent magnet embrace [16].

This work is licensed under a Creative Commons Attribution 4.0 License. For more information, see https://creativecommons.org/licenses/by/4.0/

This article has been accepted for publication in IEEE Access. This is the author's version which has not been fully edited and
content may change prior to final publication. Citation information: DOI 10.1109/ACCESS.2025.3604649

The embrace parameter influences both the back-emf voltages and the cogging torque; therefore, determining its optimal value is essential [26]. In permanent magnet machines, the embrace determines the total cost and torque characteristics. In addition, the embrace value is directly proportional to the magnet volume and has a decisive influence on torque and efficiency [27]. This value usually varies between 0.5-1 and refers to the coverage rate of the magnet rotor surface. Optimizing the Embrace value determines the relationship between power, efficiency, and magnet geometry [16]. Determining an embrace value appropriate to the design requirements is a complex process, and comparative simulations are needed to find the most suitable value [28]. In a generator, the magnet embrace significantly affects the sinusoidal shape of the induced voltage under no-load conditions [29]. The maximum cogging torque is heavily dependent on the parameter associated with the greatest common divisor of the rotor poles and stator slots. Furthermore, the cogging torque exhibits a sinusoidal variation with the magnet embrace, and the parameter related to the greatest common divisor of a specific number of stator slots and rotor poles can effectively contribute to the reduction of cogging torque [30].

- Offset Value

The offset value is defined as the distance of a specific point from the rotor's center, which in turn alters the surface geometry of the magnet facing the air gap. As the offset increases, the magnet's edge thickness diminishes, thereby transforming a fixed air gap into a variable one. This variation is generally preferred in generators because it brings the air gap flux density and, hence, the resulting back emf waveform closer to the sinusoidal form. In the case of operation as a motor, it is possible to reduce harmonics, cogging torque, and magnet consumption by adjusting the offset value; however, choosing an excessive offset value can lead to a reduction in the output power of the motor. Accordingly, by selecting a suitable offset, the efficiency of the motor is increased, vibration and torque fluctuations are reduced and magnet utilisation is optimised [8]. In PMSM, magnets can be either surface-mounted or internally positioned, and their geometrical configuration significantly influences motor performance [31].

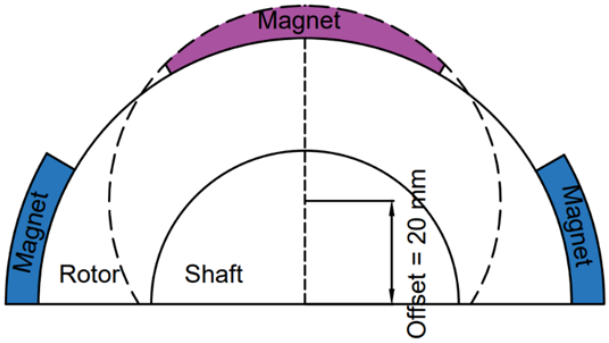

FIGURE 4. **Permanent magnet offset [8].**

- Skew

In PMSM, the stator is usually formed from laminations with the same properties, with a stepped angle in the axial direction [32].

The curvature factor can be calculated by Equation (7).

$$K = \frac{\propto_{skew}}{\propto_{slot\ pitch}} \tag{7}$$

where; K is the stator slot skew factor, $\propto_{skew}$ is the slot skew angle and $\propto_{slot\ pitch}$ is the stator slot pitch angle.

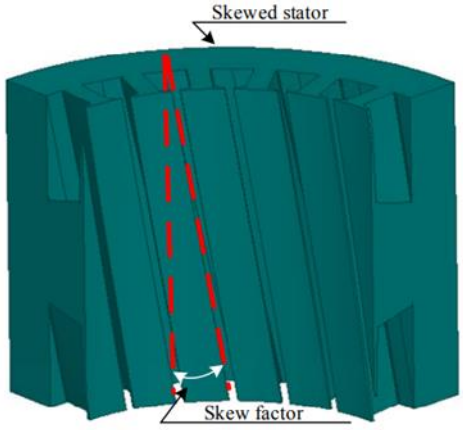

FIGURE 5. **Skewed stator geometry [25].**

It is generally accepted that a PMSM with a skewed stator will reduce both vibration and acoustic noise. In general, tilting the stator of a PMSM is effective in reducing vibration and acoustic noise. In this design, the stator slots are deflected at an angle in the axial direction to provide a more even distribution of magnetic forces. The skew factor (K) determines the stator skew and varies between 0 and 1: When K = 0, the slots are straight, when K = 1, they are axially offset by a full slot step. A skewed stator reduces vibration, while excessive skew can cause manufacturing difficulties and torque losses. Therefore, the optimum K value is a critical parameter for motor performance.

In certain motors with identical structure and configuration, the implementation of skewing can directly enhance the distribution of magnetic flux density across the air gap. In this case, the local force of the skewed stator is more uniform and balanced [25].

- Magnet Thickness

Changing the magnet thickness causes the amplitude of the air gap flux density to change and the cogging torque increases as the magnet thickness increases. Since the flux change in the air gap will also cause changes in the average output torque, the changes in the magnet thickness should be made by considering the average output torque [33]. It can be seen that magnet thickness has a linear effect on motor output

This work is licensed under a Creative Commons Attribution 4.0 License. For more information, see https://creativecommons.org/licenses/by/4.0/

This article has been accepted for publication in IEEE Access. This is the author's version which has not been fully edited and
content may change prior to final publication. Citation information: DOI 10.1109/ACCESS.2025.3604649

parameters in general, and increasing this value increases the output power and efficiency. However, increasing the magnet thickness will increase the total magnet weight, and therefore, the cost will increase [34]. As the magnet thickness increases, the rotor back-iron dimensions also change. This increases total magnet utilization, motor weight, and therefore, motor cost while increasing cogging torque and air-gap flux density. The designer's aim is to maximise efficiency while minimising the amount of magnet used, and therefore optimising the thickness of the magnet is essential [8].

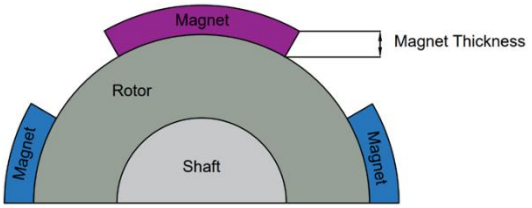

FIGURE 6. **Permanent magnet thickness.**

- Stator slot bottom width (B_{s1})

The slot geometric variables are defined as follows: hm thickness of the permanent magnet (mm), δ air gap length (mm) and H_{sw} denotes the slot opening height (mm), given by ($H_{sw} = H_{s0} + H_{s1}$). Additionally, T_{sw} is the stator tooth width (mm), H_{s0} represents the slot opening height (mm), H_{s1} is the slot shoulder height (mm) and H_{s2} corresponds to the slot depth (mm). The total slot height (mm) is given by H_s ($H_s = H_{s0} + H_{s1} + H_{s2}$). Furthermore, B_{s0} is the width of the slot opening (mm), B_{s1} is the slot bottom width (mm) and B_{s2} is the slot top width (mm).

B_{s1} of the slot is calculated by Equation (8).

$$B_{s1} = \pi \cdot \frac{D_{si}+2\cdot H_{sw}}{N_s} - T_{sw} \tag{8}$$

where, N_s represents the number of slots. The value of the slot area A_s is calculated by Equation (9).

$$A_s = \frac{(B_{s1}+B_{s2})\times(H_s+H_{sw})}{2} \tag{9}$$

Slot area A_s is an important criterion for winding placement [35], [36].

When B_{s1} changes, the diameter of the wires inside the slot also changes while the slot occupancy is constant. When the current density is variable, it is assumed that the wire diameter will change with the change of the slot area. While the current density is variable, the effect of parameter B_{s1} on the torque and torque ripple is negligible. However, reducing the wire diameter in narrow slots can lead to an increase in the resistance value and, hence, an increase in copper losses, resulting in reduced efficiency. When the slot expands, losses are reduced and efficiency increases [37].

B. OBJECTIVE FUNCTION

In this study, the analytical design problems associated with PMSM are formulated as an optimization problem, with the design process executed via optimization algorithms. In electrical machine design, critical factors such as cost (manufacturing and material costs) and thermal constraints (heat generation and cooling requirements) are also considered when determining appropriate parameters based on the user's past experience. PMSM design is considered as a complex optimisation problem from an engineering point of view and a more systematic design process is developed using mathematical models and analytical methods instead of traditional experience-based approaches. The basis of this process is Equation (10), which expresses the PMSM design mathematically.

$$Minimize\ f_{obj}(X) \quad \& \quad Subject\ to\ \{g(X) \le 0 \tag{10}$$

where, $f_{obj}(X)$ is the objective function, $g(X)$ is the inequality constraints and X is the vector containing the design variables. Table II outlines the boundary values of the design variables. Furthermore, the objective function without a penalty used in PMSM design optimization is presented in Equation (11). The total penalty function is provided in Equation (12), and the complete objective function is shown in Equation (13).

$$F_1 = ((100 - Eff)/2) + ((abs(0.5 - SSFF))/0.5) + ((abs(15000 - P_{out}))/15000) \tag{11}$$

where; F_1 is the objective function without penalty; Eff is efficiency; $SSFF$ is stator slot fill factor and P_{out} is output power.

$$T_P = Eff_p + P_{outp} + SSFF_p + STFD_p + PMW_p + T_{cogp} \tag{12}$$

where T_P is total penalty; Eff_p is efficiency penalty; P_{outp} is output power penalty; $SSFF_p$ is stator slot fill factor penalty; $STFD_p$ is stator teeth flux density penalty; PMW_p is permanent magnet weight penalty and T_{cogp} is cogging torque penalty.

$$F_{obj}(X) = F_1 + T_P \tag{13}$$

where, F_{obj} is objective function and T_P is total penalty.

The inequality constraints in the following equations are established by considering the basic parameters affecting the steady and transient state behaviour of the PMSM and are determined to ensure stable and reliable operation of the motor.

$$\begin{aligned} g_1 &= 1.8 - B_{st} \le 0 \\ g_2 &= 0.5 - SSFF \le 0 \\ g_3 &= 500 - T_{cog} \le 0 \ \ and \ \ g_3 = T_{cog} - 200 \le 0 \\ g_4 &= 15000 - P_{out} \le 0 \ \ and \ \ g_4 = P_{out} - 15000 \le 0 \\ g_5 &= Eff - 85 \le 0 \\ g_6 &= 2.5 - PMW \le 0 \end{aligned} \tag{14}$$

This work is licensed under a Creative Commons Attribution 4.0 License. For more information, see https://creativecommons.org/licenses/by/4.0/

This article has been accepted for publication in IEEE Access. This is the author's version which has not been fully edited and
content may change prior to final publication. Citation information: DOI 10.1109/ACCESS.2025.3604649

where; B_{st} is teeth flux density.

When PMSMs are evaluated in terms of performance, their high efficiency alone is not enough [38]. Therefore, in the optimization process, parameters affecting the performance, such as stator tooth flux density, stator slot occupancy rate, cogging torque, output power, and permanent magnet weight, were used as inequality constraints.

The stator teeth flux density value inequality constraint is to prevent the core from operating in saturation. Cogging torque inequality constraint is to keep the vibration and noise affecting the performance to remain at a certain level. Magnet weight is selected as the inequality constraint because it affects cost, magnet structure, efficiency, and torque. During the optimization process, the stator slot fill factor was kept close to 50%.

The block diagram summarizing the optimization process of the designed PMSM using the developed algorithm is presented in Figure 7.



FIGURE 7. Schematic diagram of the optimization process.

III. PROPOSED OPTIMIZATION ALGORITHM (fFDBGBO)

A. GRADIENT-BASED ALGORITHM (GBO)

Ahmadianfar et al. introduced a novel optimization algorithm in 2020 which was called gradient-based algorithm (GBO) [18]. The algorithm introduced in this study is influenced by Newton's search methodology and incorporates the Gradient-Based Search Rule (GSR) alongside Local Escape Operators (LEO). These operators are structured to accelerate convergence toward the optimal solution.

The fundamental role of the GSR operator is to increase exploration capability by leveraging a gradient-based mechanism and to enhance the convergence speed for attaining more favorable positions (vectors) within the search domain [39]. Accordingly, Equation (15) is employed to adjust the current vector position.

$$X1_n^m = \begin{matrix} x_n^m - randn \times \rho_1 \times \dfrac{2\Delta x \times x_n^m}{(x_{worst} - x_{best} + \varepsilon)} \\ +rand \times \rho_2 \times (x_{best} - x_n^m) \end{matrix} \quad (15)$$

where; $X1_n^m$ represents the new vector, while x_n^m denotes the current vector. $randn$ is a randomly generated number within the range [0,1], and ε a small value in the range of [0,0.1]. ρ_1 a factor used to balance the exploration and escape phase, whereas ρ_2 is a randomly chosen parameter. Δx represents the difference between the best position (x_{best}) and a randomly selected position (x_{r1}^m). In Equation (15), x_{best} replaces the current vector x_n^m, resulting in the formation of a new vector $X2_n^m$ [40].

The LEO operator, the second component of the proposed GBO algorithm, has been designed to enhance exploitation capabilities and boost efficiency by mitigating the risk of being trapped in local optima. This operator plays a crucial role in adjusting the solution's position dynamically.

LEO generates a solution, denoted as X_{LEO}^m, with improved performance by integrating multiple solutions, including the best-found position $x_{best}, X_1^{mn}, X_2^{mn}$, as well as two randomly selected solutions x_{r1}^m and x_{r2}^m, along with a newly generated candidate solution X_k^m [18].

The following expressions update X_{LEO}^m with *rand*, a random number, according to certain conditions.

$$X_{LEO}^m = \begin{matrix} X_n^{m+1} + f_1 \times (u_1 \times x_{best} - u_2 \times x_k^m) \\ +f_2 \times \rho_1 \times (u_3 \times (X2_n^m - X1_n^m) \\ +u_2 \times (x_{r1}^m - x_{r2}^m))/2 \end{matrix} \quad (16)$$

$$X_{LEO}^m = \begin{matrix} x_{best} + f_1 \times (u_1 \times x_{best} - u_2 \times x_k^m) \\ +f_2 \times \rho_1 \times (u_3 \times (X2_n^m - X1_n^m) \\ +u_2 \times (x_{r1}^m - x_{r2}^m))/2 \end{matrix} \quad (17)$$

Here; f_1 represents a uniformly distributed random variable in the interval [-1,1], while f_2 follows a normal distribution with a mean 0 and a standard deviation 1. The term pr represents probability, and corresponds to three independently generated random numbers u_1, u_2, and u_3.

B. FITNESS-DISTANCE BALANCE

In the GBO algorithm employs a greedy selection strategy to choose candidate solutions from the population to guide the search process. However, due to this method, diversity disappears quickly. In order to eliminate this situation and increase diversity, the fFDB method was developed based on the FDB selection method, which improves the intermediate performance of MHS algorithms [20].

In the GBO algorithm, the matrix equations of the m-dimensional population P consisting of n solution candidates and the vector F representing the fitness values of the solution candidates are expressed by equation (18) [41].

$$P = \begin{bmatrix} p_1 \\ \vdots \\ p_n \end{bmatrix} = \begin{bmatrix} x_{11} & \cdots & x_{1m} \\ \vdots & \ddots & \vdots \\ x_{n1} & \cdots & x_{nm} \end{bmatrix}_{nxm}, \quad F = \begin{bmatrix} f_1 \\ \vdots \\ f_n \end{bmatrix}_{nx1} \quad (18)$$

Assume that the best candidate solution in the population is represented by the vector P_{best}. Equation (19) is used to calculate the Euclidean distance of each candidate solution in P to P_{best} [42]. In this equation $x = [1, \dots, n]$ and $P_x \neq P_{best}$.

$$D_{P_x} = \sqrt{\begin{matrix} \left(P_{x[1]} - P_{best[1]}\right)^2 + \left(P_{x[2]} - P_{best[2]}\right)^2 \\ + \cdots + \left(P_{x[m]} - P_{best[m]}\right)^2 \end{matrix}} \quad (19)$$

The distance vector D_P, which represents the distance of individuals in the population to P_{best}, is as in equation (20).

This work is licensed under a Creative Commons Attribution 4.0 License. For more information, see https://creativecommons.org/licenses/by/4.0/

This article has been accepted for publication in IEEE Access. This is the author's version which has not been fully edited and
content may change prior to final publication. Citation information: DOI 10.1109/ACCESS.2025.3604649

$$D_P = \begin{bmatrix} d_1 \\ \vdots \\ d_n \end{bmatrix}_{nx1} \quad (20)$$

In the FDB selection method, the fitness value of the xth solution candidate in the population P is F_x, and the FDB score (S_{P_x}) of the xth solution candidate, $\forall_{x=1}^{n} F_x \in F$ is calculated by Equation (21):

$$S_{P_x} = w * normF_x + (1 - w) * normD_{P_x} \quad (21)$$

The determination of weight coefficients for the FDB score is outlined as follows: Equation (21) defines the vector $normF_x$ as the set of normalized fitness values corresponding to the vectors in P. Similarly, the vector $normD_{P_x}$ represents the normalized distance values associated with the vectors in P.

The population's score vector, S_{FDB} is formulated in Equation (22).

$$S_{FDB} = \begin{bmatrix} S_1 \\ \vdots \\ S_n \end{bmatrix}_{nx1} \quad (22)$$

C. FUZZY FITNESS-DISTANCE BALANCE (fFDB)

The primary objective of utilizing fuzzy logic is to enhance the process through a knowledge-based rule approach rather than relying on randomness in the algorithm's development. Consequently, a selection mechanism defined by intelligence-based expert systems is employed during the optimization process, rather than individuals being randomly determined by chance in the search space. A fuzzy-based system provides a more logical method for achieving superior solutions in real-life problems within the search area. In contrast to the principles of randomness, the fuzzy rule-based system enables the algorithm to adapt dynamically to real-time circumstances [39].

Kahraman et al. used equation (21) in the FDB score calculation based on the findings derived from simulation analyses. This is because they want $normD_{P_x}$ and $normF_x$ to affect the fdb score at the same rate. However, different studies have proven that this method is not suitable and different methods have been proposed [21], [43], [44], [45].

A fuzzy logic approach is utilized in this study to compute the FDB score of the FDB method, providing notable enhancements to the optimization algorithm. For this purpose, equation (21) was transformed into a function as shown in equation (23) using the fuzzy logic method.

$$S_{fFDB} = fuzzy(normF_x, normD_{P_x}) \quad (23)$$

The index of the optimal solution within the S_{fFDB} scores derived from Equation (23) is denoted as fFDB. The FDB score obtained based on fuzzy logic was previously used as the LEO operator in equation (16) and randomly generated r1 was replaced by fFDB as shown in the following equation.

$$X_{LEO}^{m} = X_n^{m+1} + f_1 \times (u_1 \times x_{best} - u_2 \times x_k^m) + f_2 \times \rho_1 \times (u_3 \times (X2_n^m - X1_n^m) + u_2 \times (x_{fFDB}^m - x_{r2}^m))/2 \quad (24)$$

For the proposed method, fuzzy logic includes features of fuzzification, decision-making, and defuzzification as shown in Figure 8.

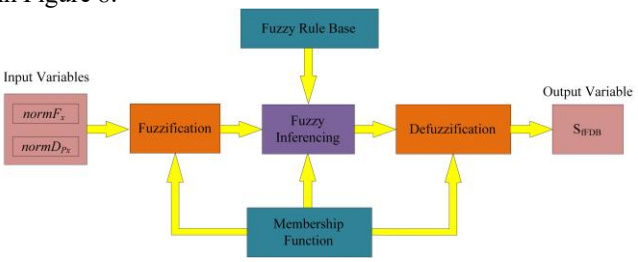

FIGURE 8. Block diagram representing the fuzzy logic system.

In this study, each input and output variable's membership function was represented using a triangular function, as shown in Figure 9.

Creating the rule base is considered to be one of the most important parts of fuzzy logic theory [39]. In order to ascertain the fuzzy logic output value, Table III displays the rule table that was developed based on user experience. This table makes it possible to use the input membership values in the planned fuzzy system to calculate the output membership function values.

In Figure 9, the labels S (small), M (medium), and B (big) serve as linguistic terms representing the membership values of both the system's inputs and outputs within the developed fuzzy logic model. Fuzzy inference rules based on this basis are presented below.

TABLE III
RULE SET FOR THE WEIGHT PARAMETER (W)

$normD_{Px}$ / $normF_x$	S	M	B
S	S	S	M
M	S	M	B
B	M	B	B

- Rule 1: if normFx is S and normDpx is S, then w is S
- Rule 2: if normFx is S and normDpx is M, then w is S
- Rule 3: if normFx is S and normDpx is B, then w is M
- Rule 4: if normFx is M and normDpx is S, then w is S
- Rule 5: if normFx is M and normDpx is M, then w is M
- Rule 6: if normFx is M and normDpx is B, then w is B
- Rule 7: if normFx is B and normDpx is S, then w is M
- Rule 8: if normFx is B and normDpx is M, then w is B
- Rule 9: if normFx is B and normDpx is B, then w is B

This work is licensed under a Creative Commons Attribution 4.0 License. For more information, see https://creativecommons.org/licenses/by/4.0/

This article has been accepted for publication in IEEE Access. This is the author's version which has not been fully edited and
content may change prior to final publication. Citation information: DOI 10.1109/ACCESS.2025.3604649

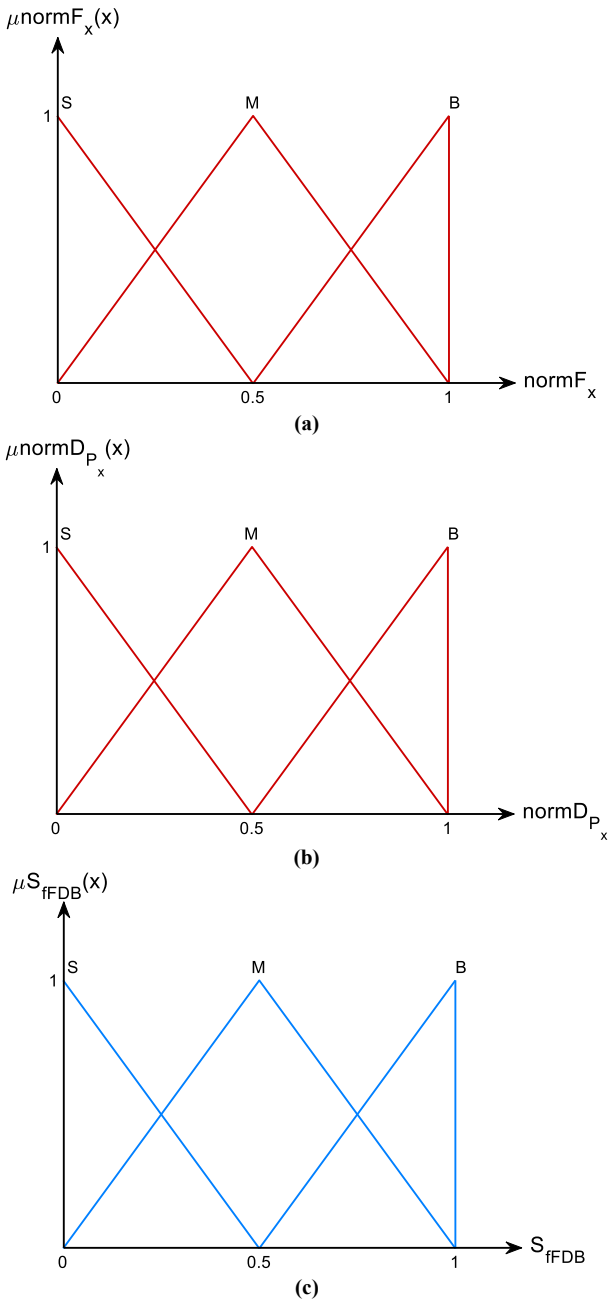

FIGURE 9. **The membership functions for the input variables are presented in (a) and (b), while that for the output variable is depicted in (c).**

The center of area defuzzification method was employed to generate a crisp output within fuzzy logic systems. The mathematical representation of this approach is provided below.

$$du = \frac{\sum_{i=1}^{n} \mu_i(du) du_i}{\sum_{i=1}^{n} \mu_i(du)} \tag{25}$$

The flowchart and pseudo code of the proposed algorithm are presented in Figure 10 and Algorithm 1.

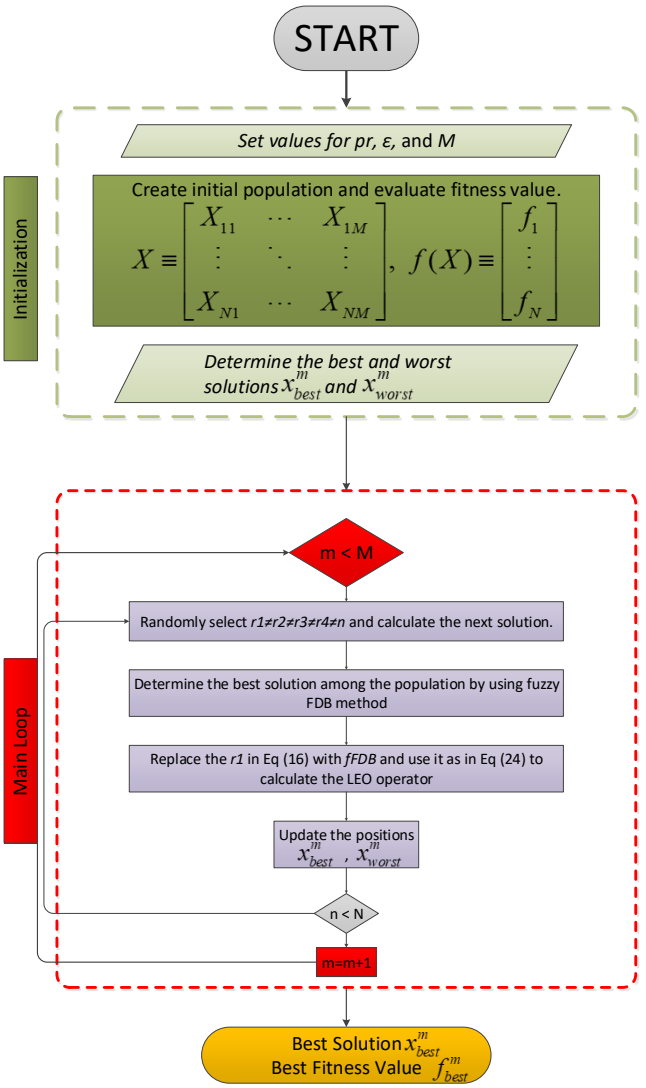

FIGURE 10. **Flowchart of the proposed algorithm.**

IV. RESULTS AND COMPARISONS

The simulation results of the fFDBGBO algorithm for the structural optimization of PMSM problem are compared with the FDBGBO, INFO, GA, PSO, ARO, DE, LSHADE, SNS, jDE, SaDE, BBO, JADE, CGBO and GBO algorithms. In the design of PMSM, five different design parameters were used. These variables are stator skew, bottom width in the slot structure, and magnet thickness, embrace and offset related to the magnet structure. These five input variables are optimized for the optimization problem, and a single objective function which is described in equation (11) is proposed.

In this study, the algorithms used in the optimization of the designed motor were run independently ten times and maximum, mean, minimum and standard deviation values were obtained. A detailed representation of these values is provided in Table IV.

According to Table IV, fFDBGBO algorithm has the mean, minimum, maximum and standard deviation values among other algorithms with the values of 0.069925, 0.069642,

This work is licensed under a Creative Commons Attribution 4.0 License. For more information, see https://creativecommons.org/licenses/by/4.0/

This article has been accepted for publication in IEEE Access. This is the author's version which has not been fully edited and
content may change prior to final publication. Citation information: DOI 10.1109/ACCESS.2025.3604649

ALGORITHM 1. Pseudocode of the proposed fFDBGBO algorithm

Step 1. Initialization
Assign values for parameters pr, ε, and M
Generate an initial population $X_0 = [X_{0,1}, X_{0,2}, \ldots, X_{0,D}]$
Evaluate the objective function $f(X_0)$, for $n = 1, \ldots, N$
Identify the best and worst solutions x_{best}^m and x_{worst}^m
Set iteration counter $m = 1$
Step 2. Main Loop
  while $(m < M)$ do
    for n = 1 to N do
      // Select individuals for candidate generation
      Randomly select $r_1 \neq r_2 \neq r_3 \neq r_4 \neq n$ in the range [1, N]
      // Determine the best solution in the population using fuzzy FDB
      Apply fuzzy FDB method to determine f_FDB
      // Replace r_1 in original Eq. (16) with fFDB and use Eq. (24) to calculate LEO
      Calculate the candidate solution using modified LEO operator
      // Local Escaping Operator
      if rand < pr then
        Calculate the position x_{LEO}^m using modified LEO Eq. (24)
        Set $x_n^{m+1} = x_{LEO}^m$
      end if
    end for
    // Update global best and worst positions
    Update x_{best}^m and x_{worst}^m
    // Increment iteration
    m = m + 1
  end while
Step 3. Return x_{best}^m and f_{best}^m

0.070418, and 0.0002414 respectively. If a more detailed analysis is made, according to the minimum fitness values, the fFDBGBO algorithm has 5.4791% better result than its closest competitor, the INFO algorithm. Additionally, when comparisons are made with other GBO variant algorithms based on the minimum fitness value, it is observed that the fFDBGBO algorithm outperformed the FDBGBO algorithm by 7.2046%, the GBO algorithm by 14.1674%, and the CGBO algorithm by 14.7119%. According to the mean of the fitness values, the fFDBGBO algorithm has 33.8276% better result than its closest competitor, the PSO algorithm.

TABLE IV
THE MAXIMUM, MEAN, MINIMUM AND STANDARD DEVIATION VALUES FOR THE OUTCOMES PRODUCED BY EACH ALGORITHM

Algorithms	Minimum	Mean	Maximum	Standard Deviation
fFDBGBO	**0.069642**	**0.069925**	**0.070418**	**0.0002414**
INFO	0.073679	0.146287	0.243839	0.0524793
GA	0.074620	0.124414	0.216448	0.0494778
FDBGBO	0.075049	0.137175	0.217901	0.0469833
PSO	0.075064	0.105671	0.171152	0.0257613
ARO	0.080077	0.125562	0.195194	0.0396684
GBO	0.081137	0.167770	0.224765	0.0526571
CGBO	0.081655	0.161867	0.219258	0.0555553
DE	0.084435	0.141485	0.208445	0.0408795
LSHADE	0.084600	0.148115	0.221992	0.0465730
SNS	0.090205	0.146225	0.197728	0.0359017
jDE	0.095242	0.139476	0.180081	0.0272489
SaDE	0.101284	0.133607	0.196329	0.0269008
BBO	0.110591	0.181766	0.223847	0.0376695
JADE	0.114813	0.143954	0.197845	0.0310222

When comparing the fFDBGBO algorithm to other GBO variant algorithms based on the mean fitness value, it is evident that the fFDBGBO algorithm outperforms the FDBGBO algorithm by 49.025%, the CGBO algorithm by 56.801%, and the GBO algorithm by 58.3209%. From another point of view, in addition to the minimum fitness value, the algorithm's having a minimum standard deviation value is also an important factor in terms of showing the robustness of the algorithm. The proposed algorithm has a standard deviation value of 0.0002414, which is lower than other algorithms, indicating that the algorithm is robust.

After ten trials with the original design and optimization technique, the control parameter values in Table V indicate the best fitness values.

Furthermore, Figure 11 illustrates the convergence curve graphs depicting the best fitness values of the algorithms under comparison. Upon analyzing the convergence curve graphs, it is evident that the proposed algorithm not only commenced with admirable results in the initial phase but also achieved the best solution in a short time frame. As an additional statistical assessment, a Friedman statistical analysis was performed using the fitness values derived from ten individual runs to statistically rank the algorithms. The Friedman score values obtained are displayed in Table VI. Upon analyzing the data in the table, the results derived from the objective function, which integrates three distinct performance metrics, indicate that the proposed fFDBGBO algorithm is the superior method, exhibiting substantial differences.

This work is licensed under a Creative Commons Attribution 4.0 License. For more information, see https://creativecommons.org/licenses/by/4.0/

This article has been accepted for publication in IEEE Access. This is the author's version which has not been fully edited and content may change prior to final publication. Citation information: DOI 10.1109/ACCESS.2025.3604649

TABLE V
CONTROL PARAMETER VALUES AND CORRESPONDING MINIMUM FITNESS VALUES OF DESIGN PROBLEM

Algorithm	Embrace	Offset	Skew	Magnet Thickness	Bs1	Minimum Fitness
Initial	0.93000	0.07900	0.85000	8.95000	5.90000	0.192627
fFDBGBO	0.92000	7.80000	0.50571	6.57971	7.07192	**0.069642**
INFO	0.90634	8.05016	0.50796	6.57747	7.10052	0.073679
GA	0.86379	5.40222	0.37979	6.49967	7.12078	0.074620
FDBGBO	0.76634	6.31260	0.64258	6.70440	7.09670	0.075049
PSO	0.76625	6.31282	0.64281	6.70475	7.09684	0.075064
ARO	0.78365	1.63524	0.70824	6.48686	7.17311	0.080077
GBO	0.86478	9.93037	0.00000	6.65908	7.15437	0.081137
CGBO	0.97212	5.00941	0.63974	6.39040	7.18763	0.081655
DE	0.64133	4.51219	0.64830	6.99984	7.08599	0.084435
LSHADE	0.88163	6.15439	0.59719	6.48349	7.21773	0.084600
SNS	0.72371	11.0665	0.53656	6.91539	7.15642	0.090205
JDE	0.72199	4.39130	0.62513	6.65855	7.27417	0.095242
SaDE	0.64006	1.32545	0.72151	6.84791	7.26212	0.101284
BBO	0.80093	7.35137	0.41876	6.52310	7.43104	0.110591
JADE	0.68268	9.13386	0.20602	6.83753	7.37232	0.114813

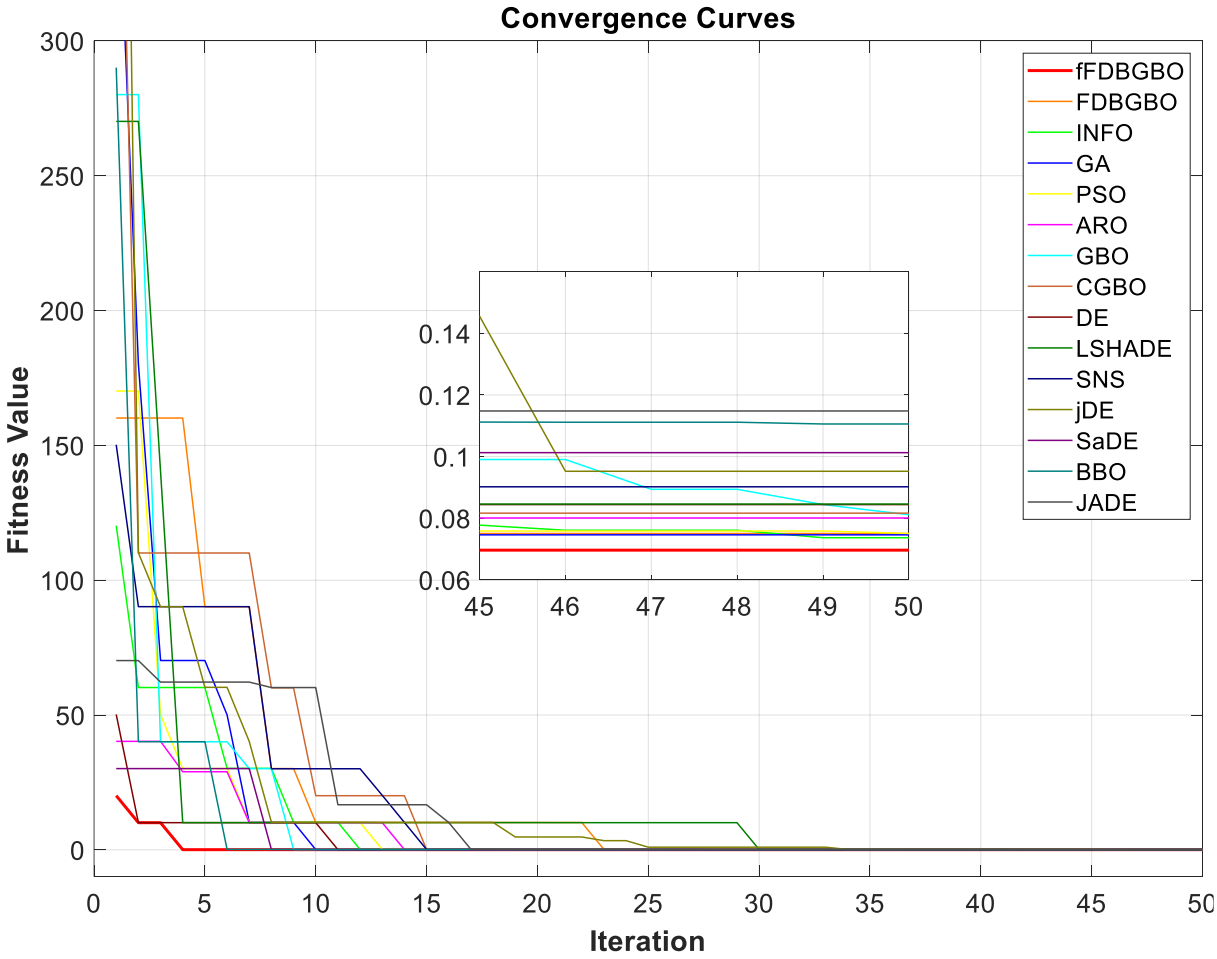

FIGURE 11. Convergence curve graphs of algorithms.

This work is licensed under a Creative Commons Attribution 4.0 License. For more information, see https://creativecommons.org/licenses/by/4.0/

This article has been accepted for publication in IEEE Access. This is the author's version which has not been fully edited and
content may change prior to final publication. Citation information: DOI 10.1109/ACCESS.2025.3604649

TABLE VI
THE FRIEDMAN STATISTICAL ANALYSIS OF ALGORITHMS

Algorithms	Friedman Score	Algorithms	Friedman Score
fFDBGBO	1	DE	7.9
INFO	8.2	LSHADE	9.2
GA	6.7	SNS	8.6
FDBGBO	7.9	jDE	8.3
PSO	4.6	SaDE	8.6
ARO	6.7	BBO	12.4
GBO	10.8	JADE	8.9
CGBO	10.2		

Furthermore, the Friedman ranking indicates that the PSO, ARO, GA, FDBGBO and DE algorithms are ranked subsequent to the suggested method in that sequence.

Computational complexity analysis was performed to see how fast the suggested algorithm works, in addition to the full performance assessments that were shown in previous analyses. When the algorithms were executed on a computer with an AMD Ryzen 5 5600X processor and 16 GB of RAM, the average time required to sustain each iteration was obtained, as shown in Table VII. The results show that the suggested fFDBGBO method takes 368.145 seconds for each iteration, which is only 1.9% longer than the basic GBO algorithm (361.244 seconds). The FDBGBO variant adds 1.2% more work, while the CGBO only adds 0.4% extra effort. As seen in performance evaluations, fuzzy logic integration makes solutions a lot better and helps them come together, but it does need quite a bit of additional effort. The fuzzy FDB technique, which is based on fuzzy logic and is calculated once for each iteration, and the fFDB method both add to the computation time. The proposed development methods do not increase the number of fitness function evaluations that are looked at during the process; hence, the computing time does not change much. The increase in computation time is minimal when compared to the significant improvement in performance.

In the models used in the initial design and developed with optimization algorithms, the properties of the slot bottom width (Bs1) and magnet geometry are discussed in detail. In this process, the structural parameters of slot bottom width and magnet geometry were optimized to increase the design's efficiency and performance. In particular, by taking into account factors such as the placement, thickness, shape and position of the magnets and the slot bottom width, the optimum structure on the electromagnetic field distribution and flux density was tried to be obtained.

TABLE VII
AVERAGE TIME PER ITERATION FOR GBO VARIANT ALGORITHMS

Algorithms	Avr. Time per Iteratıon (seconds)
fFDBGBO	368.144806
FDBGBO	365.463723
CGBO	362.525513
GBO	361.243700

The cross-section of the magnet geometry and stator slot structure of the models produced using the initial design and optimization algorithms are illustrated in detail in Figure 12.

Finite Element Analysis (FEA) was applied to the motor models created in accordance with the design parameters extracted by optimization algorithms. By using this analysis method in electrical machines, electrical and electromagnetic quantities can be obtained with high accuracy. Figure 13 shows the flux density distributions and flux lines obtained from the analysis of the designed motors. Analyses were performed on ¼ model using master-slave boundary conditions.

When the flux distributions in the part cross-section are evaluated considering the selected core material, it is seen that all models are appropriate. Although a higher flux was obtained as expected, especially in the slot tooth sections, it remained within the saturation limit. Table VIII presents additional performance metrics for the motors.

This study investigated the effect of fFDBGBO algorithm on motor performance and compared it with other algorithms. The results show that fFDBGBO provides the best performance with 93.03% efficiency and offers significant improvements in motor design by maintaining a good balance with cogging torque (434.66 mNm) and stator yoke flux density (1.4651 T) values. In the comparisons, the DE algorithm exhibited low efficiency despite offering lower cogging torque, while the JADE algorithm offered the lightest design but lagged behind in terms of efficiency and magnetic performance.

The variation of cogging torque depending on the rotor position is given in Figure 14. The lowest cogging torque value is obtained with the parameters determined by the DE optimisation algorithm, while the initial design has the highest value. fFDBGBO algorithm provides a successful optimisation by providing a balanced cogging torque profile.

V. CONCLUSIONS

Enhancing the performance of electrical machines to meet their intended applications is imperative. Moreover, the performance of electric motors can be further improved through adjustments to their parameters. In this study, the performance of a 4-pole surface-mounted 15 kW PMSM is optimized with FDBGBO, INFO, GA, PSO, ARO, DE, LSHADE, SNS, jDE, SaDE, BBO, JADE, CGBO, GBO, and fFDBGBO algorithms by considering the specified inequality constraint criteria. Taking the designed motor as a reference, a total of five values, three values of the magnet structure, stator skew, and Bs1 value of the stator slot, were optimized with 15 algorithms, taking into account their physical limits. The flux density and flux line distributions of the motors were obtained through FEA. In this study, all algorithms were executed ten times, and the results include the maximum, mean, minimum and standard deviation values from these ten runs.

This work is licensed under a Creative Commons Attribution 4.0 License. For more information, see https://creativecommons.org/licenses/by/4.0/

This article has been accepted for publication in IEEE Access. This is the author's version which has not been fully edited and content may change prior to final publication. Citation information: DOI 10.1109/ACCESS.2025.3604649



FIGURE 12. **Motor structures designed by the initial design and optimization algorithms.**

This work is licensed under a Creative Commons Attribution 4.0 License. For more information, see https://creativecommons.org/licenses/by/4.0/

This article has been accepted for publication in IEEE Access. This is the author's version which has not been fully edited and
content may change prior to final publication. Citation information: DOI 10.1109/ACCESS.2025.3604649

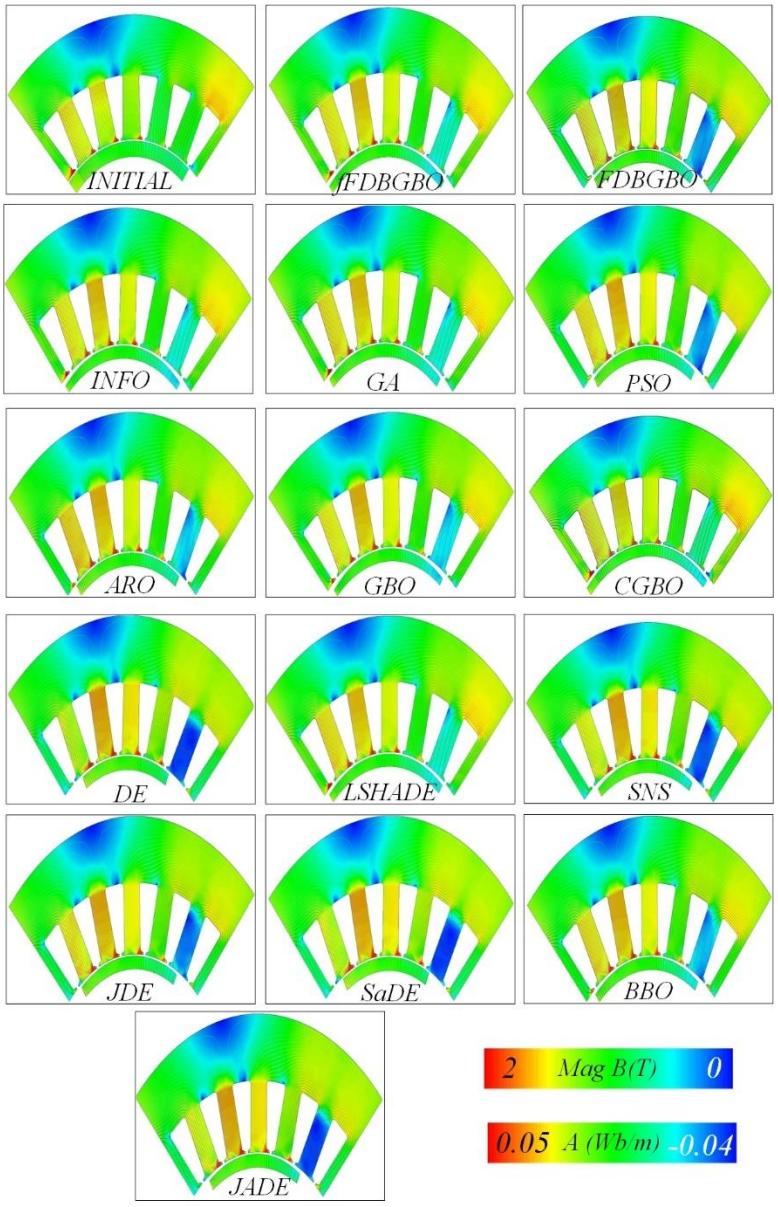

FIGURE 13. **Flux distributions and flux line distributions of motor models.**

The proposed fFDBGBO algorithm shows a 0.2979% increase in efficiency compared to the GBO algorithm for which it was developed. Compared to the initial motor design, the efficiency of the motor design obtained with the fFDBGBO algorithm was increased from 91,7788% to 93.0366%, while the magnet weight decreases from 2.14837 kg to 2.09475 kg. These results show that the fFDBGBO algorithm optimizes motor design by keeping critical parameters such as weight and fill factor within boundary values while increasing efficiency and reducing the magnet weight. In optimization algorithms, it is desired that the fitness value converges to zero. The proposed algorithms best fitness result with a value of 0.069642 shows that it has the minimum fitness value compared to other algorithms.

A single objective function with output power, stator slot fill factor and efficiency is proposed in the intended optimisation problem. With the developed fFDBGBO algorithm, the optimization results of the motor parameters in our objective function are satisfactorily improved. Thanks to the innovative approach introduced by the fFDBGBO algorithm, significant improvements were achieved in the targeted efficiency, output power, and slot fill factor parameters of the motor. The results of this study provide a comprehensive overview in terms of comparing the effects of different optimization algorithms on motor performance and provide a new perspective on the algorithms used in PMSM design.

In this study, it is possible to develop the proposed algorithm in various ways in the future. Firstly, different algorithms can be developed for the optimization of motor parameters, and

This work is licensed under a Creative Commons Attribution 4.0 License. For more information, see https://creativecommons.org/licenses/by/4.0/

This article has been accepted for publication in IEEE Access. This is the author's version which has not been fully edited and
content may change prior to final publication. Citation information: DOI 10.1109/ACCESS.2025.3604649

these algorithms can be experimentally tested. Although a general approach has been adopted in the current study, more specific solutions can be developed in the future by considering special models and constraints for each type of motor. Thus, customized objective functions can be created according to the different goals of the designers and the application areas of the motors.

Combining the proposed fuzzy logic approach with other optimization methods to enhance the algorithm's effectiveness is also a topic worth investigating. Especially by creating hybrid models with machine learning techniques, both convergence speed and solution quality can be improved. Such hybrid approaches can enhance the algorithm's ability to adapt, providing more flexible solutions to different types of problems.

In the current study, it has been observed that the algorithm yields successful results in real-life problems. This situation indicates that the algorithm is not limited to motor design but can also be used in other engineering fields. In the future, the performance of the algorithm can be tested on more complex and large-scale problems such as energy systems, optimal power flow, or the optimization of control systems. Especially in situations requiring multi-objective optimization, examining how the algorithm behaves would be beneficial.

Finally, strengthening the theoretical foundations of the algorithm is also an important topic for future research. By conducting a mathematical analysis of the convergence behavior and examining its sensitivity to different parameters, it can be more clearly understood under which conditions the algorithm performs better. Such theoretical studies will provide a solid foundation for the future development of the algorithm.

TABLE VIII
PERFORMANCE OF THE DESIGNED MOTORS

Algorithm	Efficiency (%)	Cogging Torque (mNm)	Stator Slot Fill Factor (%)	Stator Teeth Flux Density (T)	Permanent Magnet Weight (kg)	Stator yoke flux density (T)	Output Power (kW)	Total Net Weight (kg)
Initial	92.1170	316.990	56.1512	1.60921	3.19990	1.71138	15.0115	54.6316
fFDBGBO	93.0366	434.661	49.9996	1.62944	2.09475	1.46510	15	54.0436
INFO	92.9355	400.225	49.8483	1.63119	2.06129	1.44445	15	54.0027
GA	93.0562	410.924	49.7409	1.63178	2.04441	1.44863	15	54.0088
FDBGBO	92.7583	369.325	49.8684	1.63673	1.88084	1.30033	15	53.7764
PSO	92.7578	369.420	49.8679	1.63673	1.88076	1.30019	15	53.7762
ARO	93.0643	406.283	49.4640	1.63688	1.95609	1.38684	15	53.9102
GBO	92.7603	347.351	49.5630	1.63575	1.95323	1.35854	15	53.8490
CGBO	93.0603	421.747	49.3871	1.62769	2.23376	1.57750	15	54.2195
DE	91.7065	316.009	49.9250	1.64421	1.69822	1.13026	15	53.4880
LSHADE	93.0846	317.612	49.2277	1.63522	2.05078	1.45467	15	53.9934
SNS	91.8747	318.965	49.5524	1.64153	1.75280	1.18134	15	53.5533
JDE	92.6196	425.638	48.9281	1.64480	1.80683	1.25340	15	53.6684
SaDE	91.8870	343.322	48.9923	1.65035	1.69621	1.14724	15	53.4913
BBO	92.7495	383.473	48.0957	1.64648	1.87371	1.32268	15	53.7407
JADE	91.7037	304.595	48.4075	1.65084	1.68691	1.14475	15	53.4544

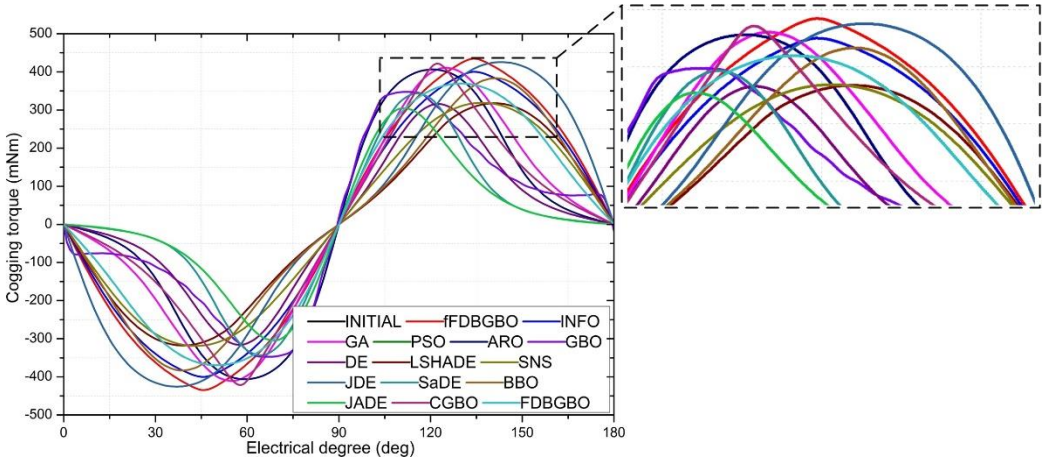

FIGURE 14. **Variation of cogging torque with rotor position.**

This work is licensed under a Creative Commons Attribution 4.0 License. For more information, see https://creativecommons.org/licenses/by/4.0/

This article has been accepted for publication in IEEE Access. This is the author's version which has not been fully edited and
content may change prior to final publication. Citation information: DOI 10.1109/ACCESS.2025.3604649

REFERENCES

[1] Vlachou, V.I.; Sakkas, G.K.; Xintaropoulos, F.P.; Pechlivanidou, M.S.C.; Kefalas, T.D.; Tsili, M.A.; Kladas, A.G. Overview on Permanent Magnet Motor Trends and Developments. Energies 2024, 17, 538. https://doi.org/10.3390/en17020538

[2] Li, Y.; Zou, J.; Lu, Y. Optimum design of magnet shape in permanent-magnet synchronous motors. IEEE transactions on magnetics 2003, 39, 3523-3526. https://doi.org/10.1109/TMAG.2003.819462

[3] Boztaş, G.; Yıldırım, M.; Aydoğmuş, Ö. Design and optimization of a PMSM for obtaining high-power density and high-speed. Turkish Journal of Science and Technology 2020, 15, 61-70.

[4] Abdalmagid, M.; Sayed, E.; Bakr, M.; Emadi, A. Geometry and topology optimization of switched reluctance machines: A review. IEEE Access 2022, 10, 5141–5170. https://doi.org/10.1109/ACCESS.2022.3149679

[5] Araz, H. K.; Yilmaz, M. Design procedure and implementation of a high-efficiency PMSM with reduced magnetmass and torque-ripple for electric vehicles. Journal of the Faculty of Engineering and Architecture of Gazi University 2020, 35, 1089-1109. https://doi.org/10.17341/gazimmfd.458515

[6] Mutluer, M.; Bilgin, O. Design optimization of PMSM by particle swarm optimization and genetic algorithm. 2012 International Symposium on Innovations in Intelligent Systems and Applications. IEEE 2012, 1-4. https://doi.org/10.1109/INISTA.2012.6247024

[7] Gan, X. G.; Fan, Z. N.; Li, J. C. Analysis of electromagnetic performance of the interior permanent magnet brushless DC motor with stator slot skewed structure based on quasi-3D moving electromagnetic-field circuit coupling calculation. Archives of Electrical Engineering 2022, 71, 159-174. https://doi.org/10.24425/aee.2022.140203

[8] Duman, S.; Dalcalı, A. Optimum design of slot and magnet structure of permanent magnet synchronous generator with teaching-learning-studying-based optimization. International Journal of Numerical Modelling: Electronic Networks, Devices and Fields 2024, 37, e3193. https://doi.org/10.1002/jnm.3193

[9] Zhang, S.; Yan, H.; Yang, L.; Zhao, H.; Du, X.; Zhang, J. Optimization Design of Permanent Magnet Synchronous Motor Based on Multi-Objective Artificial Hummingbird Algorithm. Actuators 2024, 13, 243. https://doi.org/10.3390/act13070243

[10] Sun, X.; Wan, B.; Lei, G.; Tian, X.; Guo, Y.; Zhu, J. Multiobjective and multiphysics design optimization of a switched reluctance motor for electric vehicle applications. IEEE Transactions on Energy Conversion 2021, 36(4), 3294–3304. https://doi.org/10.1109/TEC.2021.3092429

[11] Mahmouditabar, F.; Baker, N. J. Design optimization of induction motors with different stator slot rotor bar combinations considering drive cycle. Energies 2023, 17(1), 154. https://doi.org/10.3390/en17010154

[12] Asanuma, T.; Kanno, Y. Multi-objective surrogate optimization of mixed-variable IPM motor design problem with ADMM-based approach. Optimization and Engineering 2025, 1–26. https://doi.org/10.1007/s11081-025-09824-z

[13] Hong, G.; Wei, T.; Ding, X. Multi-objective optimal design of permanent magnet synchronous motor for high efficiency and high dynamic performance. IEEE Access 2018, 6, 23568-23581. https://doi.org/10.1109/ACCESS.2018.2828802

[14] Lim, D. K.; Yi, K. P.; Jung, S. Y.; Jung, H. K.; Ro, J. S. Optimal design of an interior permanent magnet synchronous motor by using a new surrogate-assisted multi-objective optimization. IEEE Transactions on Magnetics 2015, 51, 1-4. https://doi.org/10.1109/TMAG.2015.2449872

[15] Pompermaier, C.; Sjöberg, L.; Nord, G. Design and optimization of a permanent magnet transverse flux machine. 2012 XXth International Conference on Electrical Machines 2012, 606-611. https://doi.org/10.1109/ICElMach.2012.6349932

[16] Yılmaz, C.; Yenipınar, B.; Sönmez, Y.; Ocak, C. Optimization of PMSM design parameters using update meta-heuristic algorithms. Artificial Intelligence and Applied Mathematics in Engineering Problems, Springer, Cham ICAIAME 2019, 43, 914-934. https://doi.org/10.1007/978-3-030-36178-5_81

[17] Ahandani, M. A.; Abbasfam, J.; Kharrati, H. Parameter identification of permanent magnet synchronous motors using quasi-opposition-based particle swarm optimization and hybrid chaotic particle swarm optimization algorithms. Applied Intelligence 2022, 52, 13082-13096. https://doi.org/10.1007/s10489-022-03223-x

[18] Ahmadianfar, I.; Bozorg-Haddad, O.; Chu, X. Gradient-based optimizer: A new metaheuristic optimization algorithm. Information Sciences 2020, 540, 131-159. https://doi.org/10.1016/j.ins.2020.06.037

[19] Abd Elminaam, D.S.; Ibrahim, S.A.; Houssein, E.H.; Elsayed, S.M. An efficient chaotic gradient-based optimizer for feature selection. *IEEE Access* **2022**, *10*, 9271–9286. https://doi.org/10.1109/ACCESS.2022.3143802

[20] Kahraman, H. T.; Aras, S.; Gedikli, E. Fitness-distance balance (FDB): a new selection method for meta-heuristic search algorithms. Knowledge-Based Systems 2020, 190, 105169. https://doi.org/10.1016/j.knosys.2019.105169

[21] Kahraman, H. T.; Bakir, H.; Duman, S.; Katı, M.; Aras, S.; Guvenc, U. Dynamic FDB selection method and its application: modeling and optimizing of directional overcurrent relays coordination. Applied Intelligence 2022, 52, 4873–4908. https://doi.org/10.1007/s10489-021-02629-3

[22] Liu, C.; Wang, X.; Wang, S.; Wang, Y.; Lei, G.; Zhu, J. Magnetothermal coupling analysis of permanent magnet claw pole machine using combined 3D magnetic and thermal network method. IEEE Transactions on Applied Superconductivity 2022, 32(6), 1–5. https://doi.org/10.1109/TASC.2022.3154775

[23] Dalcalı, A.; Akbaba, M. Optimum pole arc offset in permanent magnet synchronous generators for obtaining least voltage harmonics. Scientia Iranica 2017, 24, 3223-3230. https://doi.org/10.24200/sci.2017.4357

[24] Aksöz, A.; Saygın, A. Aynı fiziksel ve elektromanyetik parametreler altında EASMSM ve ORSMSM'un vuruntu torkuna göre karşılaştırılması. Gazi University Journal of Science Part C: Design and Technology 2018, 6, 659-667. https://doi.org/10.29109/http-gujsc-gazi-edu-tr.400070

[25] Han, Z.; Liu, J.; Gong, C.; Lu, J. Influence mechanism on vibration and noise of PMSM for different structures of skewed stator. 2017 20th International Conference on Electrical Machines and Systems (ICEMS) 2017, 1-5. https://doi.org/10.1109/ICEMS.2017.8056025

[26] Arslan, S.; İskender, İ. Design of frameless gimbal motor for UAV applications. International Journal on Technical and Physical Problems of Engineering 2022, 14, 142-148.

[27] Izanlo, A., Gholamian, S. A., & Abdollahi, S. E. Optimal design of a permanent magnet synchronous motor for high efficiency and low cogging torque. International Journal on Electrical Engineering and Informatics 2020, 12, 173-186. https://doi.org/10.15676/ijeei.2020.12.2.1

[28] Ocak, C.; Tarimer, I.; Dalcali, A.; Uygun, D. Investigation effects of narrowing rotor pole embrace to efficiency and cogging torque at PM BLDC motor. TEM Journal 2016, 5, 25-31.

[29] Liu, T.; Huang, S.; Deng, Q.; Pu, Q.; Huang, K. Effect of the number of slots per pole on performance of permanent magnet generator direct-driven by wind turbine. 2011 International Conference on Electrical Machines and Systems 2011, 1-4. https://doi.org/10.1109/ICEMS.2011.6073738

[30] Mishra, A. K.; Rajpurohit, B. S.; Kumar, R. Revampment of surface permanent magnet synchronous motor design for ameliorated torque profile in e-mobility applications. IET Electrical Systems in Transportation 2021, 11, 99-108. https://doi.org/10.1049/els2.12007

[31] He, C.; Wu, T. Analysis and design of surface permanent magnet synchronous motor and generator. Ces transactions on electrical machines and systems 2019, 3, 94-100. https://doi.org/10.30941/CESTEMS.2019.00013

[32] Xia, C.; Zhang, Z.; Geng, Q. Analytical modeling and analysis of surface mounted permanent magnet machines with skewed slots. IEEE Transactions on Magnetics 2014, 51, 1-8. https://doi.org/10.1109/TMAG.2014.2364156

[33] Yılmaz, K.; Dindar, T. Radyal Akılı Sabit Mıknatıslı Senkron Motorlarda Vuruntu Momentinin Azaltılması. International Journal of

This work is licensed under a Creative Commons Attribution 4.0 License. For more information, see https://creativecommons.org/licenses/by/4.0/

This article has been accepted for publication in IEEE Access. This is the author's version which has not been fully edited and
content may change prior to final publication. Citation information: DOI 10.1109/ACCESS.2025.3604649

Engineering Research and Development 2023, 15, 547-557. https://doi.org/10.29137/umagd.1235442
[34] Ocak, C. Doğrudan Tahrikli Asansör Sistemlerinde Kullanılan Sabit Mıknatıslı Senkron Motorlarda Mıknatıs Geometrisinin Motor Performansı ve Maliyeti Üzerindeki Etkilerinin İncelenmesi. Mühendislik Bilimleri ve Tasarım Dergisi 2019, 7, 825-834. https://doi.org/10.21923/jesd.515050
[35] Libert, F.. Design, optimization and comparison of permanent magnet motors for a low-speed direct-driven mixer. Licentiate Thesis, Royal Institute of Technology, Stockholm, 2004.
[36] Meier, S. Theoretical design of surface-mounted permanent magnet motors with field-weakening capability. Master, Departement of Electrical Engineering, Royal Institute of Technology, Stockholm, 2002.
[37] Gündoğdu, T. Kalıcı Mıknatıslı Vernier Makinaların Parametrik Analizi, Politeknik Dergisi 2023, 1-1.
[38] Yenipinar, B.; Şahin, A.; Sönmez, Y.; Yilmaz, C.; Kahraman, H. T. Design optimization of induction motor with FDB-based Archimedes optimization algorithm for high power fan and pump applications. In The International Conference on Artificial Intelligence and Applied Mathematics in Engineering Cham: Springer International Publishing 2021, 1, 409-428. https://doi.org/10.1007/978-3-031-09753-9_29
[39] Serrano-Guerrero, J.; Romero, F. P.; Olivas, J. A. Fuzzy logic applied to opinion mining: a review. Knowledge-Based Systems 2021, 222, 107018. https://doi.org/10.1016/j.knosys.2021.107018
[40] Kadkhodazadeh, M.; Farzin, S. A novel LSSVM model integrated with GBO algorithm to assessment of water quality parameters. Water Resources Management 2021, 35, 3939-3968. https://doi.org/10.1007/s11269-021-02913-4
[41] Aydemir, S. B. Ideal solution candidate search for starling murmuration optimizer and its applications on global optimization and engineering problems. The Journal of Supercomputing 2024, 80, 4083-4156. https://doi.org/10.1007/s11227-023-05618-0
[42] Taşci, D. A.; Kahraman, H. T.; Kati, M.; Yilmaz, C. Improved gradient-based Optimizer with dynamic fitness distance balance for global optimization problems. The International Conference on Artificial Intelligence and Applied Mathematics in Engineering. Cham: Springer International Publishing 2021, 1, 247-269. https://doi.org/10.1007/978-3-031-09753-9_20
[43] Duman, S.; Kahraman, H. T.; Kati, M. Economical operation of modern power grids incorporating uncertainties of renewable energy sources and load demand using the adaptive fitness-distance balance-based stochastic fractal search algorithm. Engineering Applications of Artificial Intelligence 2023, 117, 105501. https://doi.org/10.1016/j.engappai.2022.105501
[44] Kahraman, H. T.; Hassan, M. H.; Katı, M., Tostado-Véliz, M.; Duman, S.; Kamel, S. Dynamic-fitness-distance-balance stochastic fractal search (dFDB-SFS algorithm): an effective metaheuristic for global optimization and accurate photovoltaic modeling. Soft Computing 2024, 28, 6447-6474. https://doi.org/10.1007/s00500-023-09505-x
[45] Ozkaya, B., Guvenc, U., & Bingol, O. (2022). Fitness Distance Balance based LSHADE algorithm for energy hub economic dispatch problem. IEEE Access, 10, 66770-66796.



HASAN UZEL received the B.Sc. degree from the Department of Electrical-Electronics Engineering, Faculty of Engineering, Ondokuz Mayıs University, Samsun, in 1997, and the M.Sc. degree from the Department of Electrical Education, Institute of Science, Gazi University, Ankara, Turkey, in 2006, respectively. He has been studying as a Ph.D. student at the Department of Electrical and Electronics Engineering, Institute of Science, Duzce University, Duzce, Since 2019. He worked as a lecturer at Akdağmadeni Vocational School, Sivas University, between 1997 and 2006, and he has been working at Akdağmadeni Vocational School, Yozgat Bozok University, since 2006. His research interests include electrical machines, optimization, and power systems.



YUNUS HINISLIOGLU received the B.Sc. degree from the Department of Electrical-Electronic Engineering, Faculty of Engineering-Architecture, Meliksah University, Kayseri, Turkey, in 2015, and the M.Sc. and Ph.D. degrees from the Department of Electrical-Electronic Engineering, Institute of Science, Duzce University, Duzce, Turkey, in 2019 and 2024, respectively. He has been working as a Research Assistant with the Department of Electrical-Electronic Engineering, Duzce University, since 2016. His research interests include power systems, optimization, and renewable energy sources.



ADEM DALCALI received the B.Sc. and M.Sc. degrees from Gazi University, Ankara, Turkey, in 2010 and 2013, respectively, and the Ph.D. degree in electric and electronics engineering from Karabük University, Karabük, Turkey, in 2017. From 2013 to 2017, he was a Research Assistant with the Department of Electric and Electronics Engineering, Karabük University. He is currently an Associate Professor with the Department of Electrical-Electronics Engineering, Bandırma Onyedi Eylül University, Bandırma, Turkey. His research interests include wind energy and the numerical analysis of the electromagnetic field in electrical machinery.

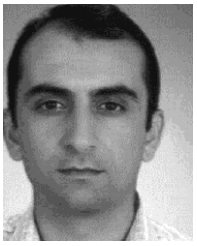

UGUR GUVENC received the B.Sc. degree from the Department of Electrical Education, Faculty of Technical Education, Duzce University, Duzce, Turkey, in 2002, and the M.Sc. and Ph.D. degrees from the Department of Electrical Education, Institute of Science and Technology, Gazi University, Ankara, Turkey, in 2006 and 2008, respectively. He has worked as a Research Assistant with the Department of Electrical Education, Gazi University, from 2003 to 2008; a Research Assistant with the Department of Electrical Education, Duzce University, from 2008 to 2010; and an Assistant Professor, from 2010 to 2014, and an Associate Professor, from 2014 to 2019, with the Department of Electrical and Electronics Engineering, Duzce University. He is currently a Professor with the Department of Electrical and Electronics Engineering, Duzce University. Besides that, he took on several administrative tasks, such as the Vice Dean, the Head of the Department of Electrical and Electronics Engineering, the Head of the Department of Electrical Education, and the Head of the Research and Application Center. He has more than 100 publications, including articles. His research interests include power systems, optimization, artificial intelligence, and renewable energy sources.

This work is licensed under a Creative Commons Attribution 4.0 License. For more information, see https://creativecommons.org/licenses/by/4.0/